PNAS

Supporting Information for

Senolytic and senomorphic agent procyanidin C1 alleviates structural and functional decline in aged retina

Yidan Liu[a,1], Xiuxing Liu[a,1], Xuhao Chen[a,1], Zhenlan Yang[a,1], Jianqi Chen[a], Weining Zhu[b], Yangyang Li[a], Yuwen Wen[a], Caibin Deng[a], Chenyang Gu[a], Jianjie Lv[a], Rong Ju[a], Yehong Zhuo[a,*], Wenru Su[a,*]

[a]State Key Laboratory of Ophthalmology, Zhongshan Ophthalmic Center, Sun Yat-sen University, Guangdong Provincial Key Laboratory of Ophthalmology and Visual Science, Guangzhou, P. R. China

[b]Department of Clinical Medicine, Zhongshan School of Medicine, Sun Yat-sen University, Guangzhou, P. R. China

[1]These authors contributed equally to this work.

*Co-corresponding authors: Wenru Su and Yehong Zhuo

State Key Laboratory of Ophthalmology, Zhongshan Ophthalmic Center, Sun Yat-sen University, Guangdong Provincial Key Laboratory of Ophthalmology and Visual Science, Guangzhou 510060, P. R. China. Phone number: +86-20-87330402 (office), +86-13570364296 (mobile)

Email: suwr3@mail.sysu.edu.cn, zhuoyh@mail.sysu.edu.cn

Author Contributions: Yidan Liu, Wenru Su, and Yehong Zhuo conceived the study. Yidan Liu, Xiuxing Liu, and Wenru Su contributed to the design of the experiments. Xuhao Chen, Zhenlan Yang, Jianqi Chen, Weining Zhu, Yangyang Li, Yuwen Wen, Caibin Deng, Chenyang Gu and Jianjie Lv provided study material and/or the assembly of data. Yidan Liu and Xiuxing Liu performed experiments and data collection. Yidan Liu, Xiuxing Liu, Xuhao Chen, and Zhenlan Yang contributed to data analysis and figure preparation. Yidan Liu, Xiuxing Liu, and Xuhao Chen drafted the manuscript. Rong Ju provided experimental guidance in the revision. Wenru Su and Yehong Zhuo supervised the research. Yehong Zhuo provided the financial funding. All authors reviewed and approved the manuscript.

Competing Interest Statement: No conflict of interest to declare.

Classification: Major – Biological sciences, Minor – Medical Sciences

Keywords: cellular senescence, senescence-associated secretory phenotype, senolytics, aging, retina

This PDF file includes:

Supplementary Table 1-3

Materials and methods

Animals and drug treatment

The wild-type C57BL/6J male mice were purchased from Guangdong Medical Laboratory Animal Center. All animals were raised in a pathogen-free facility in the Animal Laboratories of Zhongshan Ophthalmic Center. The Institutional Animal Care and Use Committee of Zhongshan Ophthalmic Center, Sun Yat-sen University, approved the experiments. All mice were housed in a 12-hour light/dark cycle. The mice were divided into the following three groups: (1) Young group with 6- to 8-week-old mice received standard water and food ad libitum. (2) Aged group with 14- to 16-month-old mice received standard water and food ad libitum. (3) PCC1 group with 14- to 16-month-old mice received water and tailor-made food ad libitum. PCC1 (#E0478, Selleck, Houston, TX, USA) was mixed with the regular chow with a concentration of 8 mg/kg, which was an approximate average dosage of 3.2mg/kg·d for each mouse. The administration of PCC1 lasted for four months before euthanasia.

Ultra-performance liquid chromatography (UPLC)

Following PCC1 treatment, the concentration of PCC1 in mouse retina was determined using UPLC. To enable HPLC analysis, the collected samples, along with a PCC1 standard (#E0478, Selleck, Houston, TX, USA), were prepared according to a standardized protocol for detection using ACQUITY UPLC® (Waters, Milford, MA, USA).

Immunofluorescence staining

Mice were anesthetized with 1% isoflurane and transcardially perfused with 0.9% saline solution and 4% paraformaldehyde (PFA). The whole eyeballs were harvested and postfixed in 4% PFA at 4°C for 2 hours. Tissue dehydration was performed overnight using 30% sucrose. Subsequently, the tissues were embedded in optimal cutting temperature compound (SAKURA, Japan) and cryosectioned into 14-μm-thick slices. The sections were permeabilized by 0.3% Triton X-100 and blocked by 2% bovine serum albumin with 10% normal donkey serum. The samples were then incubated with primary antibodies at 4 °C overnight and a species-compatible secondary antibody for 2 hours at room temperature. The primary antibodies used were as follows: anti-GFAP (#ab194324, Abcam) at 1:500, anti-IBA1 (#019-19741, Wako) at 1:500, anti-p16 (#ab211542, Abcam) at 1:500, anti-PKC alpha (#ab32376, Abcam) at 1:100, and anti-Calbindin (#13176T, Cell Signaling Technology) at 1:100. For TdT-mediated dUTP nick end labeling (TUNEL), cells were stained using the TUNEL assay kit (#11684817910, Roche, Basel, Switzerland) according to the manufacturer's instructions. DAPI solution (Bioss, China) was used for cell nuclei staining. Images were captured by Nikon confocal microscope (C2+, Nikon, Japan) and processed by ImageJ software (https://imagej.nih.gov/ij/).

RNAscope

RNA in situ hybridization was performed using the RNAscope® multiplex fluorescent reagent kit (ACD Diagnostics, Hayward, CA, USA). Probes used were designed by the manufacturer. Briefly, fresh frozen sections of mouse eyes were first dehydrated with ethanol in a sequential gradient of 50%,70%, and two rounds of 100% for 5 min each. Subsequently, pretreatment steps involving hydrogen peroxide and protease IV were performed following the manual instructions. Probes were then applied and hybridized followed by detection utilizing TSA Vivid Fluorophore 570. Imaging was accomplished using a Nikon confocal microscope (C2+, Nikon, Japan), with subsequent processing conducted using ImageJ software (https://imagej.nih.gov/ij/).

Real-time reverse transcription-quantitative PCR (RT-qPCR)

Total RNA was extracted from mouse retina using the RN002 RNA-Quick Purification Kit (ESscience, China) according to the manufacturer's instructions. The concentration and purity of extracted RNA was measured by NanoDrop 2000 spectrophotometer (Thermo Fisher Scientific Inc., US). cDNA was synthesized with the Evo M-MLV RT Mix Kit (AGbio, China) according to its standard all-in-one protocol. Quantitative amplification of the target genes was performed with the SYBR Green Pro Taq HS Premix (AGbio, China) using the Light Cycler 480 Real-Time PCR System (Roche Molecular Systems, Inc., SUR). The expression level of target mRNAs was normalized to that of Actb (β-Actin). Primer sequences are listed in the supplementary Table 2-3.

Murine electroretinogram (ERG)

Full-field ERG recordings were performed using a Celeris D430 rodent ERG system (Diagnosys LLC, Westford, MA, USA). Briefly, after dark adaptation overnight, the mice were intraperitoneally anesthetized with pentobarbital sodium solution (100 mg/kg). The pupils were dilated with compound tropicamide eye drops for 5 min. Each mouse was placed on a platform heater at 37℃. Corneal electrodes with an integrated stimulator were simultaneously placed in both eyes after lubrication with 1–2% hydroxypropyl methylcellulose. We selected the TOUCH/TOUCH protocol for bilateral detection and used the unstimulated side as the reference. By default, the ground electrode is assumed to be unconnected in the TOUCH/TOUCH protocol. We first performed a scotopic ERG with increasing light intensities from 0.01, 0.1, 1 to 3 $cd \cdot s/m^2$. A 10-min light adaptation was then performed with a background light intensity of 30 $cd \cdot s/m^2$. Photopic ERG were subsequently recorded at 3 and 10 $cd \cdot s/m^2$. Ten sweeps were conducted for each stimulus. The pre-trigger and post-trigger times were set to 50 and 300 ms, respectively, and the sampling frequency was set to 2000 Hz. The a-wave amplitude was measured by calculating the difference between the baseline and trough, whereas the b-wave amplitude referred to the difference between the trough of the a-wave and the peak of the tallest curve.

Flow cytometry analysis

For analysis of retina, the mice retina from different groups were extracted and the cell suspensions were isolated by grinding the organs through nylon mesh. For analysis of cell lines, cells were obtained from different groups through enzyme digestion. Dead cells were excluded using live/dead dye (#423105, BioLegend, San Diego, CA, USA). Then cells were stained with the following surface antibodies: CD11B BV605 (#101237, BioLegend), CD73 PE (#127205, BioLegend) and CD90.2 BV605 (#105343, BioLegend). For intracellular markers staining, cells were stimulated with 5 ng/mL of phorbol myristate acetate, 500 ng/mL ionomycin, and 1 mg/mL brefeldin A (Sigma) at 37 °C for 5 h, following by fixation and permeabilization. Then, cells were stained with the following antibodies: IL-6 PE (#504504, BioLegend), TNF-α BV421 (#506327, BioLegend), IL-1β PE-Cy7 (#25-7114-80, Invitrogen, Carlsbad, CA, USA) and p21 Alexa Fluor 647 (#ab237265, Abcam, Cambridge, MA, USA) for mouse retina as well as BV2 cells, IL-6 PE-Cy7 (#501119, BioLegend), p53 PE (#645806, BioLegend), p21 Alexa Fluor 488 (#ab282187, Abcam, Cambridge, MA, USA) for HRMEC. For the p16 staining, cells were stained with surface antibodies, fixed, permeabilized, stained with p16 antibody (#ab211542, Abcam), then stained with Alexa Fluor 647-labeled antibody (#4414S, Cell Signaling Technology, Danvers, USA). To assess the specificity of the p16 antibody in flow cytometry, additional controls including isotype control (#ab172730, Abcam) and unstained controls were performed. The isotype control matches the host species and Ig subclass of the anti-p16 antibody. For the β-galactosidase (β-GAL) staining, cells were stained with the senescence assay kit (#ab228562, Abcam) according to the manufacturer's instructions. Finally, the cells were harvested and analyzed by flow cytometry. For Annexin V and Propidium iodide (PI) staining, cells were stained with the apoptosis assay kit (#556547, BD Biosciences, San Jose, CA, USA) according to the manufacturer's instructions. Finally, the cells were harvested and analyzed by flow cytometry. The flow cytometer (BD LSRFortessa, USA) was used for analysis and the results were analyzed with FlowJo software (version 10.0.7, Tree Star, Ashland, OR, USA).

Cell culture and treatment protocols

The BV2 murine microglial cell line was obtained from Zhong Qiao Xin Zhou Biotechnology Company (Shanghai, China). The human retinal microvascular endothelial cells (HRMEC), human retinal pigment epithelial cell line ARPE-19 and 661W photoreceptor cell line were acquired from American Type Culture Collection (ATCC, United States). All cell lines were cultured at 37℃ with 5% CO2 under normoxic conditions. 661W and APRE-19 cells were cultured in DMEM/F12 (Gibco) while BV2 and HRMEC cells were cultured in DMEM (Gibco). Complete medium was prepared by supplementing the respective medium with 10% fetal bovine serum and 1% penicillin/streptomycin. To induce senescence, 661W and APRE-19 cells were subjected to treatment with 200 μM H_2O_2 (#7722-84-1, Sigma-Aldrich, St. Louis, MO, USA) in complete medium for four hours daily over four consecutive days. Cells were otherwise maintained in complete medium throughout the remaining duration. Following the four-day treatment period, cells were cultured in complete medium for an additional two days before harvesting. For BV2 cells, the stimulation agent was switched from H_2O_2 to 10 ng/ml lipopolysaccharide (LPS, #297-473-0, Sigma-Aldrich). The efficacy of repeated LPS stimulation in inducing cellular senescence in BV2 cells has been confirmed in the literature (1). The treatment regimen for BV2 cells was identical to that of 661W and APRE-19 cells. To establish the in vitro diabetic retinopathy (DR) model, HRMEC cells were treated with 30 mM glucose (Beyotime, China) in complete medium for two days. The PCC1-treated groups were exposed to the agent at a concentration of 50 μM for 24 hours.

Cell viability assay

Senescent or control cells (5×10^3/well) were seeded into a 96-well plate, treated with various concentrations of PCC1 (5–200 μM), and incubated at 37°C in a humidified incubator under 5% CO_2 for 24 hours. Cell viability was determined using a Cell Counting Kit-8 (CCK8, #GK10001, GLPBIO, Montclair, CA, USA) according to the manufacturer's instructions.

Enzyme-linked immunosorbent assay (ELISA)

The serum from mice were determined using the mouse IL-1 beta ELISA Kit (#88-7013-22, invitrogen), mouse IL-6 ELISA Kit (#88-7064-88, invitrogen) and mouse TNF alpha ELISA Kit (#88-7324-88, invitrogen). For HRMEC cells, supernatants of different groups were collected at the end of incubation. Interleukin-6 (IL6) and Vascular Endothelial Growth Factor-A (VEGF-A) were measured with human IL-6 ELISA kit (#88-7066-88, invitrogen) and VEGF-A Human ELISA Kit (#BMS277-2, Invitrogen) respectively, according to manual guide.

Single-cell RNA sequencing analysis

10× Genomics kit was used to construct barcoded libraries. The sequenced data was initially processed in CellRanger (version 7.0.0) count pipeline and integrated by CellRanger aggr command. Subsequent analysis was performed in R using Seurat package (version 4.1.1)(2) with the default parameters unless otherwise specified. Cells with more than 200, fewer than 4000 genes, and less than 20% mitochondrial genes were retained after quality control. We obtained 72,054 cells after quality control (young, 37,150 cells; aged, 7,980 cells; and PCC1-treated aged mice, 26,924 cells) for downstream analysis. The R package harmony (version 0.1.0) was used to correct the batch effect of different sequencing samples. The scRNA-seq data of nAMD and DR was downloaded from Gene Expression Omnibus (GEO) database under the accession number GSE135922 and GSE178121. Metadata and expression count were imported into R to perform subsequent analysis. Differential expression analysis was performed by "FindMarkers" function integrated in Seurat. Genes with | Log2 (Fold Change) | > 0.25 and P value < 0.05 were defined as differentially expressed genes (DEGs).

Gene functional analysis

Function annotation of DEGs was conducted by Gene Ontology (GO) analysis in the Metascape (3). Several representative GO terms or pathways were demonstrated in R package ggplot2 (version 3.3.6).

Cell-cell interaction analysis

Intracellular cell-cell communication was predicted in the R package CellChat (version 1.4.0) (4). Signaling pathway across the three groups and interaction networks were visualized, and the expression of ligands and receptors was presented in violin plots.

Senescent cells identification

In order to avoid the bias, we first performed the stratified sampling of the three groups (Young, Aged, PCC1) according to the number of each cell type to ensure the same number of total cells from three groups. We then conducted gene set variation analysis (GSVA) of integrated expression matrix using “enrichit” function from R package escape (version 1.4.0) referring to the SenMayo gene set (5). Cells of top 10% ES were manually defined as senescent cells.

Gene set score analysis

Gene related to NF-κB and p38MAPK signaling pathway were downloaded from MSigDb (https://www.gsea-msigdb.org/gsea/index.jsp). Gene set scores were calculated by the Seurat function “AddModuleScore” from R package Seurat.

Statistical analysis

Data were presented as mean ± SD (standard deviation). Two-tailed Student’s t-test and Mann-Whitney U test were used for two group comparisons depending on the normality and equal variance of data. One-way ANOVA and Kruskal-Wallis test with Bonferroni post-hoc test were used for statistical analysis of variables in multiple groups depending on the normality and equal variance of data. P value < 0.05 was considered statistically significant. The sample sizes and P values were both indicated in the figure legends. The statistical analysis was performed by GraphPad Prism 9 (GraphPad Software, United States) and R software (version 4.1.3).

Data availability statement

The scRNA-seq data are deposited in the Genome Sequence Archive in BIG Data Center, Beijing Institute of Genomics (BIG, https://ngdc.cncb.ac.cn/gsa/), Chinese Academy of Sciences, under the GSA Accession No. CRA011488. The data analysis pipeline used in scRNA-seq follows the description on the 10X Genomics and Seurat official websites. The analysis steps, functions, and parameters used are described in detail in the Materials and methods section.

SI References

1. H.-M. Yu, *et al.*, Repeated Lipopolysaccharide Stimulation Induces Cellular Senescence in BV2 Cells. *Neuroimmunomodulation* **19**, 131–136 (2012).
2. A. Butler, P. Hoffman, P. Smibert, E. Papalexi, R. Satija, Integrating single-cell transcriptomic data across different conditions, technologies, and species. *Nat. Biotechnol.* **36**, 411–420 (2018).
3. Y. Zhou, *et al.*, Metascape provides a biologist-oriented resource for the analysis of systems-level datasets. *Nat. Commun.* **10**, 1523 (2019).
4. S. Jin, *et al.*, Inference and analysis of cell-cell communication using CellChat. *Nat. Commun.* **12**, 1088 (2021).
5. D. Saul, *et al.*, A new gene set identifies senescent cells and predicts senescence-associated pathways across tissues. *Nat. Commun.* **13**, 4827 (2022).

Supplementary Figure and Legend

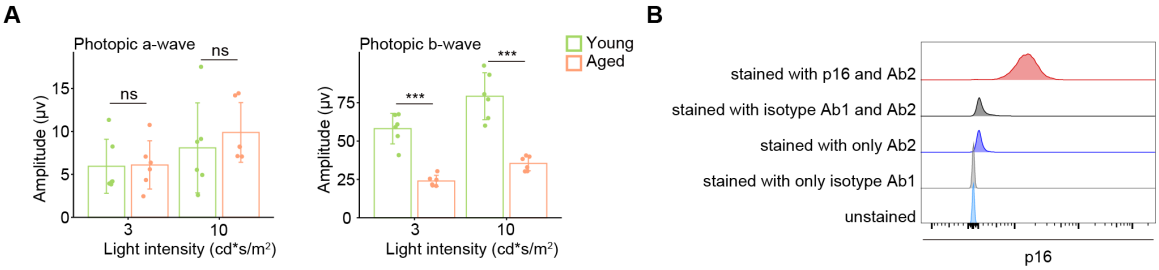

Fig. S1 The aged retina showed decreased photopic responses
A. Bar charts showing the quantification of photopic ERG amplitudes (n = 6/group). Data are shown as mean ± SD and P values were analyzed using unpaired two-tailed Student's *t*-test; ns, non-significant; ***P < 0.001.
B. To assess the specificity of the p16 antibody in flow cytometry, additional controls including isotype control and unstained controls were performed. Flow cytometry histogram showing the fluorescence of p16 in senescent BV2 cells stained with different combinations of antibodies (Abbreviations: Ab1, primary antibody; Ab2, secondary antibody).

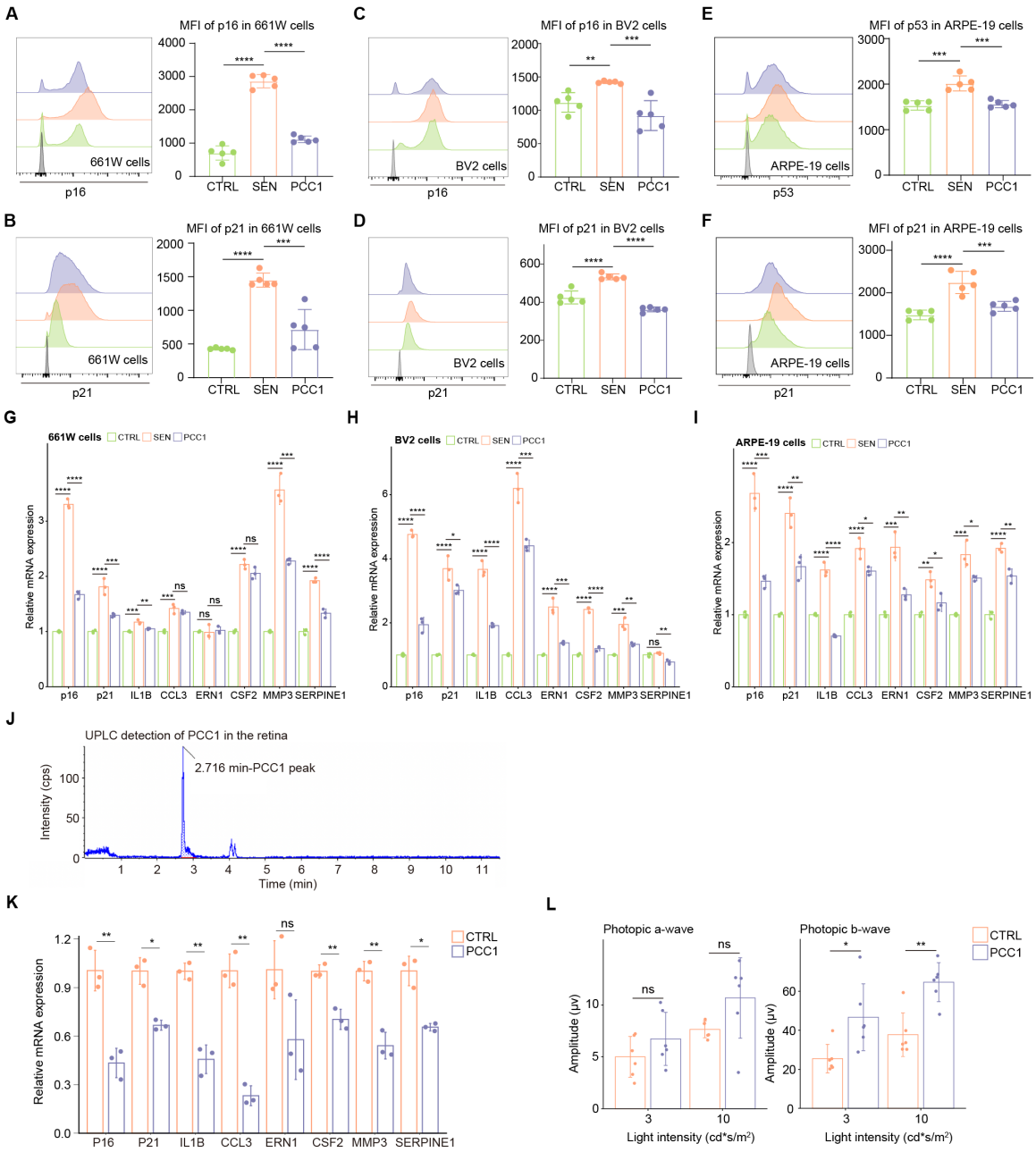

Fig. S2 Long-term PCC1 treatment relieved functional and structural impairment in aged retina by both senolytic and senomorphic effects

A-F. Representative flow charts (left) and quantification (right) of the proportion of p16 and p21 in 661W (A-B), BV2 cells (C-D), p53 and p21 in ARPE-19 cells (E-F).

G-I. Bar plots showing the relative mRNA expression levels of senescence markers and several SASP-related genes were detected by real-time quantitative PCR between control, senescent and PCC1-treated senescent groups in 661W (G), BV2 (H) and ARPE-19 (I) cells (n = 3/group).

J. UPLC analysis revealed a detectable PCC1 peak (at 2.716 min) in the retina.

K. Bar plot showing relative mRNA expression levels of several SASP-related genes were detected by RT-qPCR between control and PCC1-treated aged mice (n = 3/group).

L. Bar charts showing the quantification of photopic ERG amplitudes (n = 6/group).

Data are shown as mean ± SD. P values were analyzed using one-way ANOVA with Bonferroni post-hoc test (A-I) or unpaired two-tailed Student's *t*-test (K-L); ns, non-significant; *P < 0.05; **P < 0.01; ***P < 0.001, ****P < 0.0001.

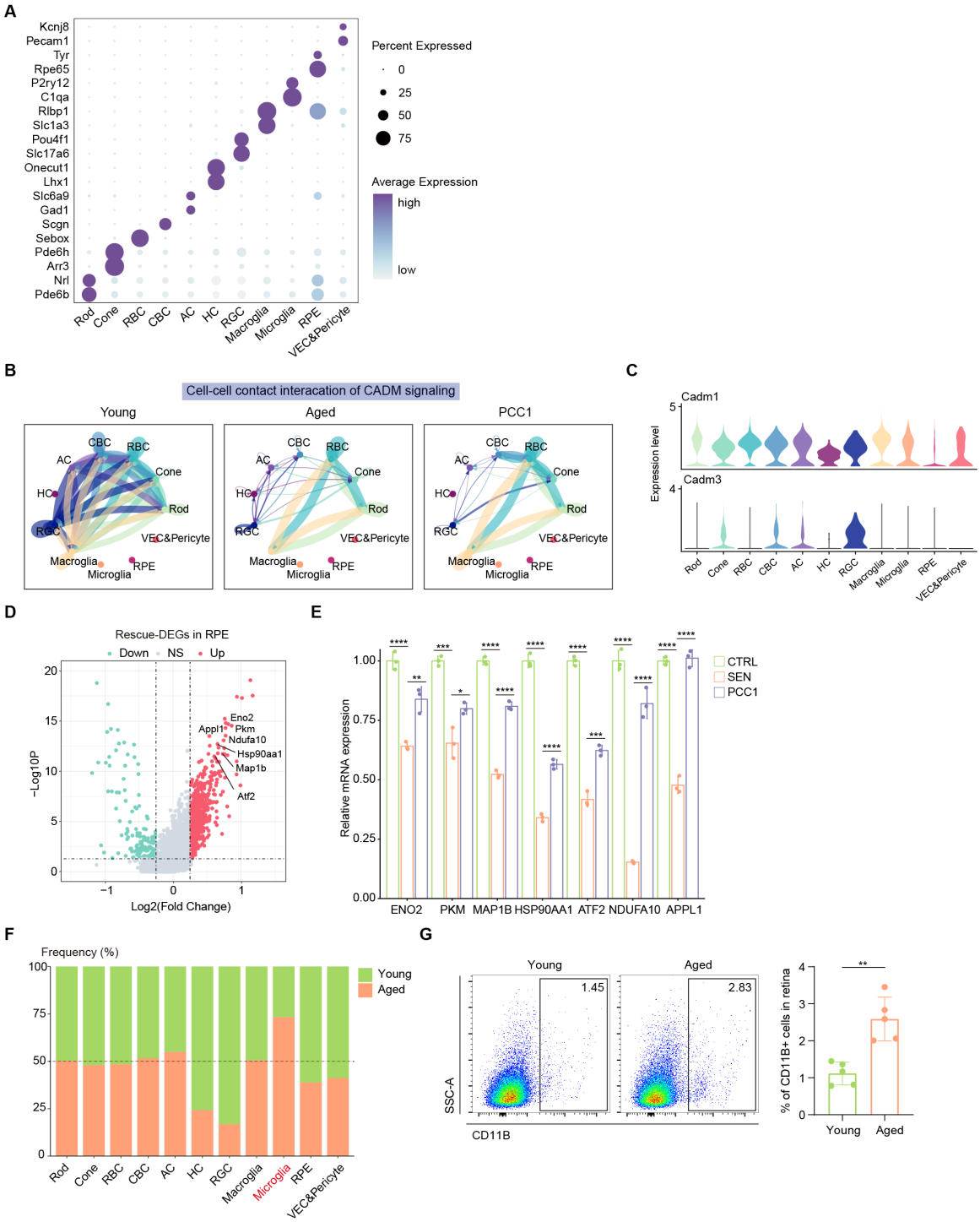

278 **Fig. S3** The seotherapeutic effects of PCC1 treatment on aged retina evaluated by single-cell
279 analysis
280 A. Dot plot showing markers genes (rows) that uniquely mark different cell types in mouse retina
281 (columns). The size of the dot indicates the percentage of cells expressing the gene, and the
282 color represents the average expression level of the gene in the indicated cell types.
283 B. Circle plots showing the inferred CADM signaling networks among three groups. Edge width
284 represents the communication probability.

C. Violin plots showing the expression of the ligand-receptor involved in the inferred CADM signaling pathway.
D. Volcano plot showing Rescue-DEGs of RPE.
E. Bar plots showing the relative mRNA expression levels of several Rescue-DEGs detected by real-time quantitative PCR between control, senescent and PCC1-treated senescent groups ARPE-19 cells (n = 3/group).
F. Bar plot showing the ratios of different retinal cell types of aged mice compared to young mice derived from scRNA-seq data.
G. Representative flow charts (left) and quantification (right) of the proportion of microglia from retina of young and aged group (n = 5/group).
Data are shown as mean ± SD. P values were analyzed using one-way ANOVA with Bonferroni post-hoc test (E) or unpaired two-tailed Student's t test (G); *P < 0.05, **P < 0.01, ***P < 0.001, ****P < 0.0001.

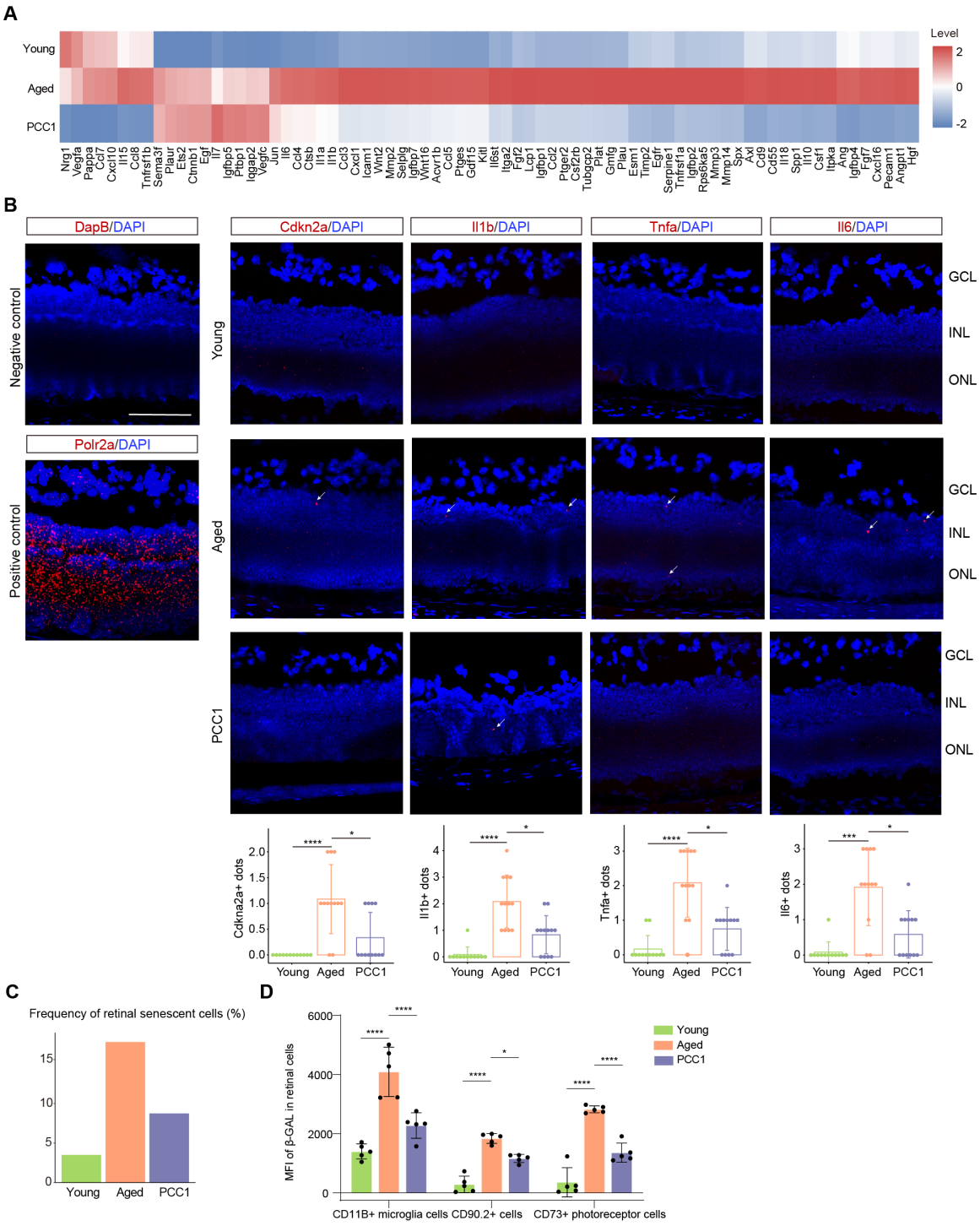

298 **Fig. S4** Senescent cells and SASP factors were reduced after PCC1 treatment
299 A. Heatmap showing the expression pattern of SASP-related genes in three groups.
300 B. Representative confocal images of RNAscope analysis of Cdkn2a, Il1b, Tnfa and Il6 on retinal
301 frozen sections from the young (upper panel), aged (middle panel) and PCC1-treated (lower
302 panel) mice (n = 6/group). The positive control was detected using the Polr2a probe and the
303 negative control was detected using the DapB probe. The arrow indicates positive cells in the
304 retina. Scale bar 100 μm.
305 C. Bar plot showing the proportions of senescent cells in various retinal cell types in the retina.

D. Bar plots showing quantification of the MFI of β-gal in CD11B+ microglia cells, CD90.2+ cells and CD73+ rod photoreceptor cells.
Data are shown as mean ± SD. P values were analyzed using Kruskal-Wallis test with Bonferroni post-hoc test (B) or one-way ANOVA with Bonferroni post-hoc test (D); *P < 0.05, ***P < 0.001, ****P < 0.0001.

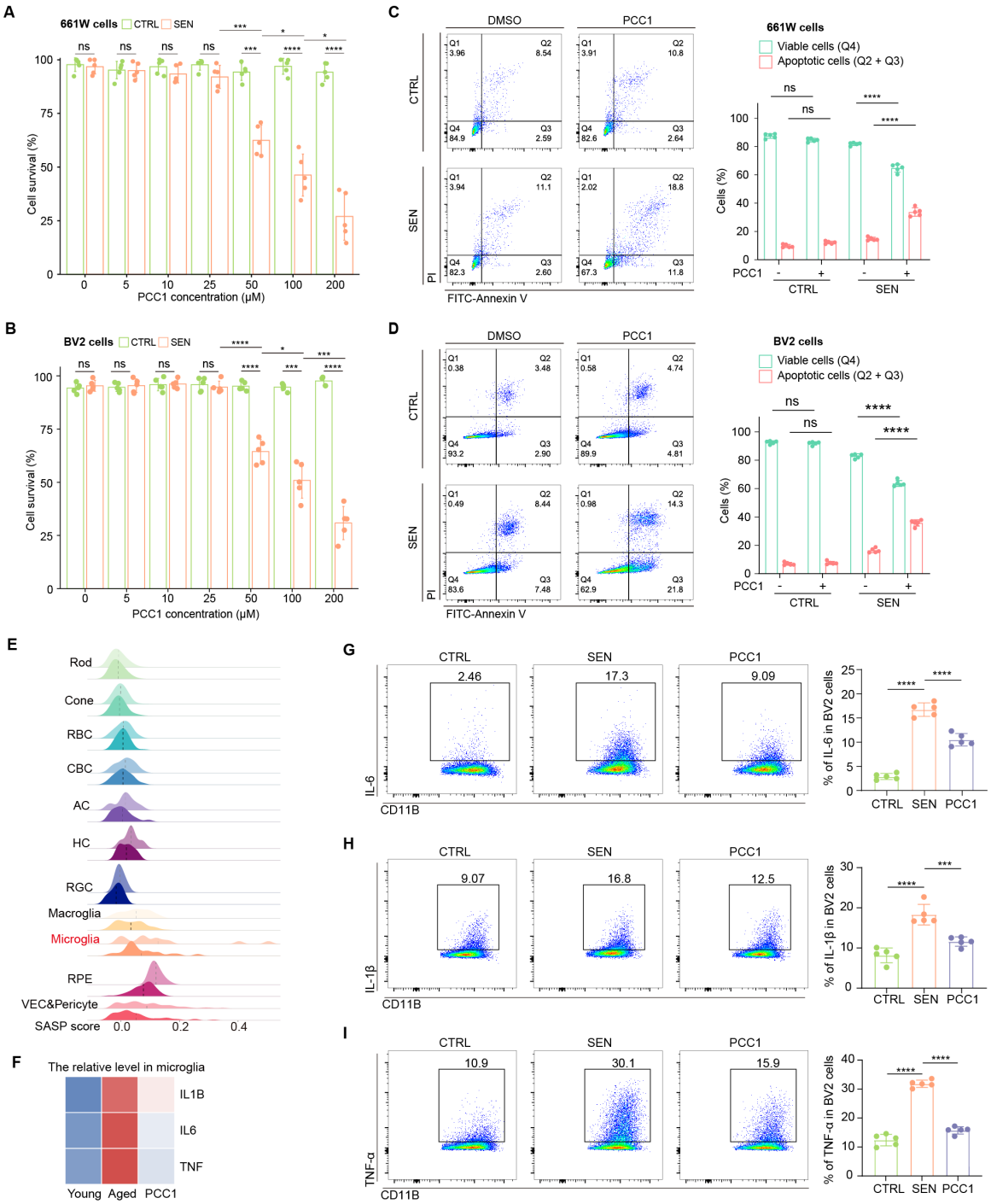

Fig. S5 Experimental validation of depletion of senescent cells both in vivo and in vitro by PCC1

A-B. Bar plot showing CCK-8 assay on control and senescent cells of 661W (A) and BV2 cell line (B) upon treatment of PCC1 (n=5/group).

C-D. Representative flow charts (left) and quantification (right) of AnnexinV/PI apoptotic assay on control and senescent cells of 661W (C) and BV2 cell line (D) upon treatment of PCC1 (n=5/group).

E. Ridge plots showing the expression of SASP factors in each cell type in retina with lighter color indicating the aged group and darker color indicating the PCC1-treated aged group. The dashed lines indicate the mean values.

F. Heatmap showing the expression level of indicated genes in micrgolia in single-cell data.

G. Representative flow charts (left) and quantification (right) of the proportion of IL-6, IL-1B and TNF-α in BV2 cells among three groups (n=5/group).
Data are shown as mean ± SD. P values were analyzed two-tailed unpaired Student's t-test (A-D) or one-way ANOVA with Bonferroni post-hoc test (G-I); ns, non-significant; *P < 0.05, ***P < 0.001, ****P < 0.0001.

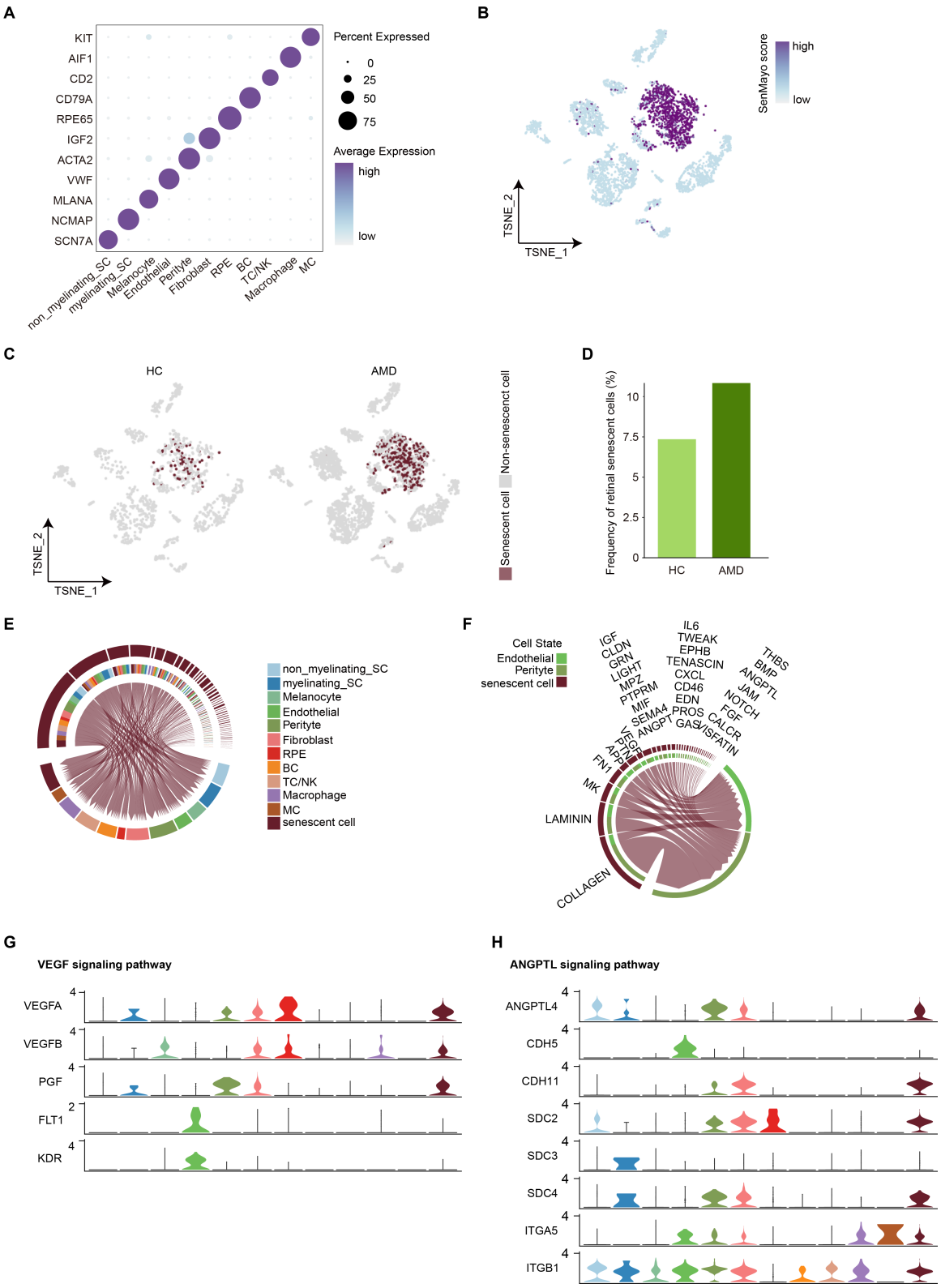

329 **Fig. S6** Cellular senescence was increased in neo-vascular age-related macular degeneration
330 **A.** Dot plot showing markers genes (rows) that uniquely mark different cell types in RPE and
331 choroid (columns). The size of the dot indicates the percentage of cells expressing the gene, and
332 the color represents the average expression level of the gene in the indicated cell type.

B. t-SNE plot showing the ES of SASP-related genes of RPE and choroidal cells.
C. t-SNE plot showing the distribution of senescent cells in the RPE and choroid between the two groups.
D. Bar plot showing the percentage of senescent cells in all retinal cells of two groups.
E. Chord plot showing the interactions between the senescent cells and target cells, including all cell types in the RPE and choroid.
F. Chord plot showing the interactions between the senescent cells and the target cells, endothelial cell and pericytes.
G. Violin plot showing the expression of the ligand-receptors involved in the inferred VEGF signaling pathway.
H. Violin plot showing the expression of the ligand-receptors involved in the inferred ANGPTL signaling pathway.

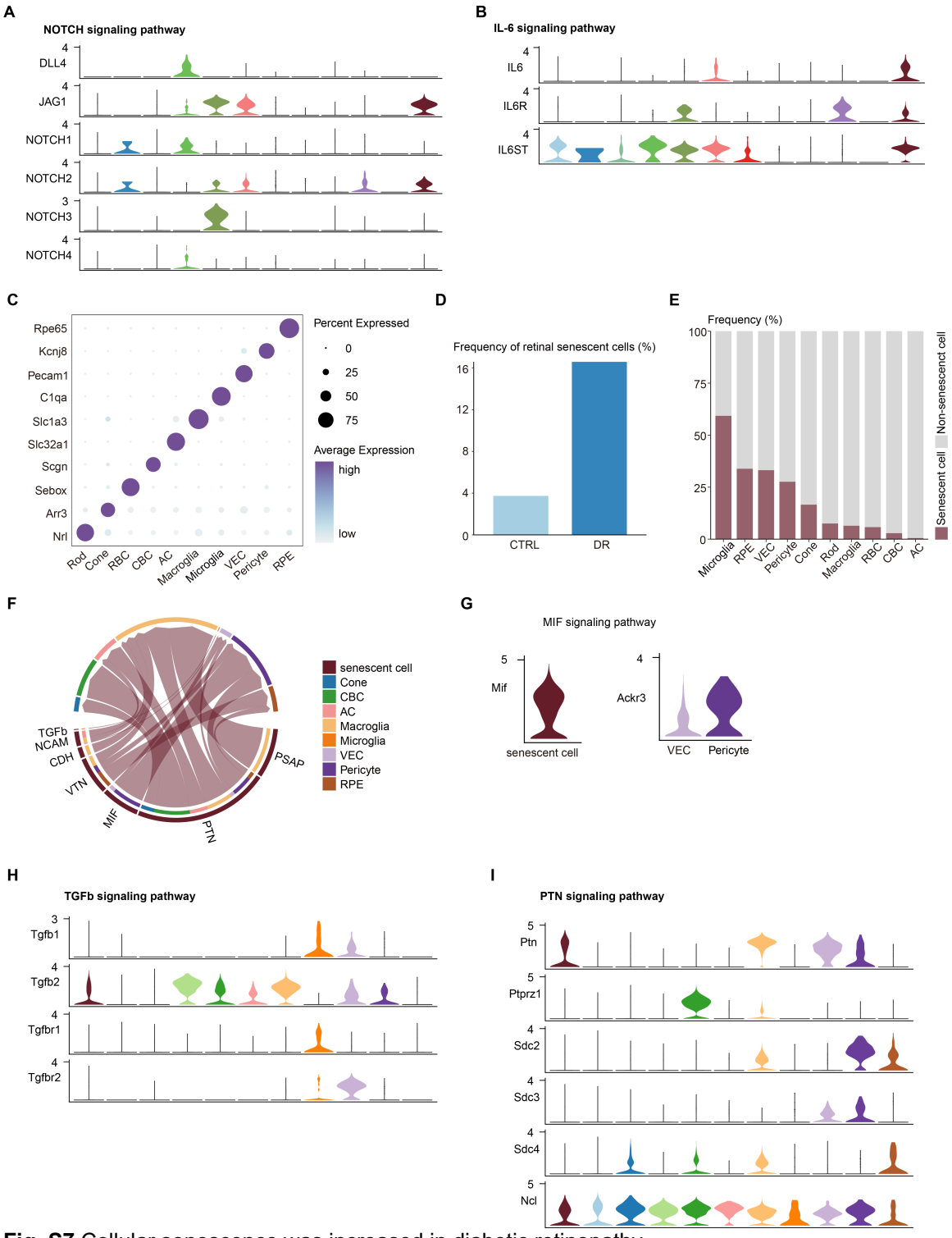

Fig. S7 Cellular senescence was increased in diabetic retinopathy
A. Violin plot showing the expression of the ligand-receptors involved in the inferred NOTCH signaling pathway.
B. Violin plot showing the expression of the ligand-receptors involved in the inferred IL-6 signaling pathway.

C. Dot plot showing markers genes (rows) that uniquely mark different retinal cell types (columns). The size of the dot indicates the percentage of cells expressing the gene, and the color represents the average expression level of the gene in the indicated cell type.
D. Bar plot showing the percentage of senescent cells in all retinal cells of two groups.
E. Bar plot showing the proportions of senescent cells in different retinal cell types in the retina.
F. Chord plot showing the interactions between the senescent cells and target cells, including all cell types in the retina.
G. Violin plot showing the expression of the ligand-receptor involved in the inferred MIF signaling pathway.
H. Violin plot showing the expression of the ligand-receptors involved in the inferred TGFb signaling pathway.
I. Violin plot showing the expression of the ligand-receptors involved in the inferred PTN signaling pathway.

Supplementary Table and Legend

Table S1. PCC1 deletes senescent cells in each cell type of retina assessed in scRNA-seq data

	A	B	C	D	E	F	G
Rod	405	4089	9.9%	373	4341	8.59%	1.31%
Cone	16	226	7.08%	11	171	6.43%	0.65%
RBC	7	51	13.73%	4	50	8%	5.73%
CBC	17	62	27.42%	13	98	13.27%	14.15%
AC	5	24	20.83%	3	15	20%	0.83%
HC	0	4	0%	0	4	0%	0%
RGC	2	6	33.33%	0	7	0%	33.33%
Macroglia	161	247	65.18%	92	212	43.4%	21.78%
Microglia	86	105	81.9%	22	61	36.07%	45.83%
RPE	237	260	91.15%	51	112	45.54%	45.61%
VEC&Pericyte	13	19	68.42%	10	22	45.45%	22.97%

A = The number of predicted senescent cells in each cell type of Aged group
B = The number of total cells in each cell type of Aged group
C = A/B = The ratio of senescent cells in each cell type of Aged group
D = The number of predicted senescent cells in each cell type of PCC1 group
E = The number of total cells in each cell type of PCC1 group
F = D/E = The ratio of senescent cells in each cell type of PCC1 group
G = C-F = Reduced ratio of senescent cells in each cell type by PCC1

Table S2. A list of mouse primer sequences for qRT-PCR assays.

Target name	Forward (5'-3')	Reverse (5'-3')
p16	GCTCAACTACGGTGCAGATTC	GCACGATGTCTTGATGTCCC
p21	CCTGGTGATGTCCGACCTG	CCATGAGCGCATCGCAATC
IL1B	GAAATGCCACCTTTTGACAGTG	TGGATGCTCTCATCAGGACAG
CCL3	TGTACCATGACACTCTGCAAC	CAACGATGAATTGGCGTGGAA
ERN1	ACACTGCCTGAGACCTTGTTG	GGAGCCCGTCCTCTTGCTA
CSF2	GGCCTTGGAAGCATGTAGAGG	GGAGAACTCGTTAGAGACGACTT
MMP3	TTGATGGGCCTGGAACAGTC	AGTCCTGAGAGATTTGCGCC
SERPINE1	TGACGTCGTGGAACTGC	GAAAGACTTGTGAAGTCGGC
ACTB	GGCTGTATTCCCCTCCAT	CCAGTTGGTAACAATGCC

383 **Table S3** A list of human primer sequences for qRT-PCR assays.

Target name	Forward (5'-3')	Reverse (5'-3')
p16	GATCCAGGTGGGTAGAAGGTC	CCCCTGCAAACTTCGTCCT
p21	TGTCCGTCAGAACCCATGC	AAAGTCGAAGTTCCATCGCTC
IL1B	ATGATGGCTTATTACAGTGGCAA	GTCGGAGATTCGTAGCTGGA
CCL3	AGTTCTCTGCATCACTTGCTG	CGGCTTCGCTTGGTTAGGAA
ERN1	CACAGTGACGCTTCCTGAAAC	GCCATCATTAGGATCTGGGAGA
CSF2	TCCTGAACCTGAGTAGAGACAC	TGCTGCTTGTAGTGGCTGG
MMP3	AGTCTTCCAATCCTACTGTTGCT	TCCCCGTCACCTCCAATCC
SERPINE1	ACCGCAACGTGGTTTTCTCA	TTGAATCCCATAGCTGCTTGAAT
ENO2	AGCCTCTACGGGCATCTATGA	TTCTCAGTCCCATCCAACTCC
PKM	ATGTCGAAGCCCCATAGTGAA	TGGGTGGTGAATCAATGTCCA
MAP1B	ATCTCGACACTCTGCAAGATTCT	CTGGTCCAAGTTGCACTCAAT
HSP90AA1	CATAACGATGATGAGCAGTACGC	GACCCATAGGTTCACCTGTGT
ATF2	AATTGAGGAGCCTTCTGTTGTAG	CATCACTGGTAGTAGACTCTGGG
NDUFA10	GTGCAAACTGCGCTATGGAAT	CAGGAAAGTGCTTGAAGCCTA
APPL1	ACTTGGGTACATGCAAGCTCA	TCCCTGCGAACATTCTGAACG
ACTB	CATGTACGTTGCTATCCAGGC	CTCCTTAATGTCACGCACGAT

384